Cent. Eur. J. Phys. • 6(1) • 2008 • 26-32
DOI: 10.2478/s11534-008-0036-y

VERSITA

Central European Journal of **Physics**

Transport behaviour of a Bose Einstein condensate in a bichromatic optical lattice

Research Article

Aranya B. Bhattacherjee[1]*, Monika Pietrzyk[2]

1 *Max Planck-Institute für Physik komplexer Systeme, Nöthnitzer Str. 38, 01187 Dresden, Germany*

2 *Weierstraß-Institut für Angewandte Analysis und Stochastik, Mohrenstr.39, 10117 Berlin, Germany*

Received 19 September 2007; accepted 30 January 2008

Abstract: We investigate the Bloch and dipole oscillations of a Bose Einstein condensate (BEC) in an optical superlattice. We show that, as the effective mass increases in an optical superlattice, the BEC is localized in accordance with recent experimental observations [J.E. Lye *et. al.* Phys. Rev. A 75, 061603 (2007)]. In addition, we find that the secondary optical lattice is a useful additional tool to manipulate the dynamics of the atoms.

PACS (2008): 03.75.Lm, 03.75.Kk

Keywords: Bose Einstein condensate • bi-chromatic optical lattice • Bloch oscillation • dipole oscllation • localization

1. Introduction

The interference of intersecting laser beams creates a periodic potential for atoms, known as an optical lattice [1]. Ultracold bosons trapped in such periodic potentials have been widely used to study some fundamental concepts of quantum physics such as Josephson effects [2], squeezed states [3], Landau-Zener tunneling and Bloch oscillations [4], and superfluid-Mott insulator transition [5]. Progress in experimental techniques has led to many interesting theoretical studies on Bloch dynamics of Bose-Einstein condensates in periodic potentials such as the prediction of a new, interaction-induced Bloch period [6], Bloch oscillations of cold atoms in two-dimensional optical lattices [7] and wavepacket analysis of the Bloch-Zener oscillations of a BEC in a periodic potential [8]. Localizing BECs increases spatial control of the atomic cloud, which can be used in many experiments and applications. Localized states of BECs in optical lattices have been predicted by Trombettoni *et al.* [9]. The dynamics of BEC in periodic potentials is governed by the discrete nonlinear Schrödinger equation which is known to support self-trapped states and travelling breathers [10]. A new technique to localize BEC in optical lattice via boundary dissipation was proposed recently by Livi *et al.* [11]. Nonlinear self trapping of matter waves in optical lattices have also been observed experimentally [12]. Nonlinear Josephson oscillations and self trapping of BEC are important fundamental concepts. They have been studied in great detail in the context of two coupled condensates and three coupled condensates. Noise thermometry with two weakly coupled BECs was investigated recently by

*E-mail: bhattach@mpipks-dresden.mpg.de

Gati *et al.* [13]. Tunneling and non-linear self trapping in a single Bosonic Josephson junction have been observed by Albiez *et al.* [14]. Theoretically in the context of two coupled BEC's, the Josephson effect, Π oscillations and macroscopic quantum self-trapping were predicted some time ago [15]. Self-trapping mechanisms in three coupled BEC's has also been extensively studied by Franzosi *et al.* [16]. Recently, Josephson oscillation and transition to self-trapping state in a triple well has also been studied [17]. An important promising application under study is quantum computation in optical lattices [18]. Optical lattices are therefore of particular interest from the perspectives of both fundamental quantum physics and its connection to applications. Using superposition of optical lattices with different periods [19], it is now possible to generate periodic potentials characterized by a richer spatial modulation, the so-called optical superlattices. The light-shifted potential of the superlattice is described as

$$V(z) = V_1 \cos^2\left(\frac{\pi z}{d_1}\right) + V_2 \cos^2\left(\frac{\pi z}{d_2} + \phi\right). \qquad (1)$$

Here d_1 and d_2 are, respectively, the primary and secondary lattice constants, V_1 and V_2 are the respective amplitudes and ϕ is the phase of the secondary lattice. When $\phi = 0$, all sites of the lattice are perfectly equivalent due to the symmetries of the system, so that the population and onsite energies are same at each site. An asymmetry is introduced when $\phi \neq 0$ and hence the onsite energies are not the same at each site.

Theoretical interest in optical superlattices started only recently. Examples include work on fractional filling Mott insulator domains [20], dark [21] and gap [22] solitons, the Mott-Peierls transition [23], non-mean field effects [24] and phase diagrams of BEC in two-color superlattices [25]. Porter *et al.* [26] have shown that optical superlattices can manipulate and control solitons in BEC. The analogue of the optical branch in solid-state physics has also been predicted in an optical superlattice [27]. Rousseau *et al.* [28] have considered the effect of a secondary lattice on a one-dimensional hard core of bosons (strongly correlated regime). A detailed theoretical study of the Bloch and Bogoliubov spectrum of a BEC in a one-dimensional optical superlattice has been done by Bhattacherjee [29]. In an interesting work [30], we show that due to the secondary lattice, there is a decrease in the superfluid fraction and the number fluctuation. The dynamic structure factor which can be measured by Bragg spectroscopy is also suppressed due to the addition of the secondary lattice. The visibility of the interference pattern (the quasi-momentum distribution) of the Mott-insulator is found to decrease due to the presence of the secondary lattice. In a very recent experiment [31], it was observed that the center-of-mass motion of a BEC is blocked in a quasi-periodic lattice. Considering the fact that these optical superlattices are now being realized experimentally and interesting experiments are being done routinely, we were motivated to study the influence of the secondary lattice on Bloch oscillations and dipole oscillations of atoms. In particular, we show that the effective mass of the BEC increases in the presence of the secondary lattice which, consequently blocks the center-of-mass motion of the BEC.

2. Bloch oscillations

We consider an elongated cigar-shaped BEC confined in a harmonic trap potential of the form $V_{ho}(r,z) = \frac{m}{2}(\omega_r^2 r^2 + \omega_z^2 z^2)$ and a one-dimensional tilted optical superlattice of the form $V_{op}(z) = E_R\left(s_1 \cos^2(\frac{\pi z}{d}) + s_2 \cos^2(\frac{\pi z}{2d})\right) + mgz$. We have taken a particular case where $d_2 = 2d_1 = 2d$. Here, s_1 and s_2 are the dimensionless amplitudes of the primary and the secondary superlattice potentials with $s_1 > s_2$. $E_R = \dfrac{\hbar^2\pi^2}{2md^2}$ is the recoil energy ($\omega_R = \dfrac{E_R}{\hbar}$ is the corresponding recoil frequency) of the primary lattice. We take $\omega_r \gg \omega_z$ so that an elongated cigar shaped BEC is formed. The harmonic oscillator frequency corresponding to small motion about the minima of the optical superlattice is $\omega_s \approx \dfrac{\sqrt{s_1}\hbar\pi^2}{md^2}$. The peak densities in each well match the Gaussian profile. Since the array is tilted, the atoms undergo coherent Bloch oscillations driven by the interwell gravitational potential mgz. The BEC is initially loaded into the primary lattice and the secondary lattice is switched on slowly. The frequency of each minima of the primary lattice is not perturbed significantly by the addition of the secondary lattice. Here $\omega_s \gg \omega_z$ so that the optical lattice dominates over the harmonic potential along the z-direction and hence the harmonic potential can be neglected. The high laser intensity will give rise to an array of several quasi-two-dimensional pancake-shaped condensates. Because of the quantum tunneling, the overlap between the wave functions of two consecutive layers can be sufficient to ensure full coherence. We study now the Bloch dynamics of the BEC in the tilted optical superlattice by solving the discrete nonlinear Schroedinger equation (DNLSE). The dynamics of the BEC is governed by the Gross-Pitaevskii equation (GPE),

$$i\hbar\frac{\partial\zeta}{\partial t} = -\frac{\hbar^2}{2m}\nabla^2\zeta + \left\{V_{ho}(r,z) + V_{op}(z) + g_0|\zeta|^2\right\}\zeta, \quad (2)$$

where $g_0 = \dfrac{4\pi\hbar^2 a}{m}$, with a the two body scattering length and m the atomic mass. In order to understand the basic physics of the system, we consider the case of a deep

optical lattice (large laser intensities), where analytic solutions can be obtained in the tight binding approximation. In this approximation, the interwell barriers are much higher than the chemical potentials. In the tight binding approximation the condensate order parameter can be written as

$$\zeta(r,t) = \sqrt{N_T}\sum_j \Psi_j(t)\phi(r-r_j), \tag{3}$$

where N_T is the total number of atoms and $\phi(r-r_j) = \phi_j$ is the condensate wavefunction localized in the trap j with $\int dr\phi_j\phi_{j+1} \approx 0$, and $\int dr\left|\phi_j\right|^2 = 1$; $\Psi_j(t)$ is the j^{th} amplitude. $\Psi_j(t) = \sqrt{\rho_j(t)}\exp(i\theta_j(t))$ where $\rho_j = \frac{N_j}{N_T}$, with N_j and θ_j being the number of particles and phases in the trap j respectively. Substituting the Ansatz (3) in (2), we find that the GPE reduces to the DNLSE,

$$i\frac{\partial\Psi_j}{\partial t} = -\frac{1}{2}\left\{\left(1-\alpha(-1)^{j-1}\right)\Psi_{j-1} + \left(1-\alpha(-1)^{j}\right)\Psi_{j+1}\right\} + \left(\varepsilon_j + \Lambda\left|\Psi_j\right|^2\right)\Psi_j. \tag{4}$$

Here $\varepsilon_j = \frac{1}{J_0}\int dr\left[\frac{\hbar^2}{2m}\left(\bar{\nabla}\phi_j\right)^2 + \left(V_{ho}(r)+V_{op}(z)\right)\left|\phi_j\right|^2\right]$, $\Lambda = \frac{g_0N_T}{J_0}\int dr\left|\phi_j\right|^4$, $\alpha = \frac{\Delta_0}{2J_0}$. One can show using $J_j = -\int dr\left[\frac{\hbar^2}{2m}\bar{\nabla}\phi_j\cdot\bar{\nabla}\phi_{j+1} + \phi_j\left(V_{ho}(r)+V_{op}(z)\right)\phi_{j+1}\right]$ that there are distinctly two Josephson coupling parameters, $J_{1,2} = J_0 \pm \frac{\Delta_0}{2}$ where $J_0 \approx \frac{E_R}{4}\left[\left(\frac{\pi^2}{2}-2\right)s_1\right]\exp\left(-\frac{\pi^2\sqrt{s_1}}{4}\right)$ and $\Delta_0 \approx \frac{E_R}{2}s_2\exp\left(-\frac{\pi^2\sqrt{s_1}}{4}\right)$ [29]. We have rescaled time as $t \to \frac{\hbar}{2J_0}t$. In Eq. (4), $\varepsilon_j = \omega_B j$, where $\omega_B = \frac{mg\lambda_1}{4J_0}$ is the frequency of Bloch oscillation and λ_1 is the wavelength of the laser creating the primary lattice. In order to understand the Bloch and dipole oscillations, we solve the DNLSE using a variational approach adopted from [9]. The Hamiltonian function corresponding to the DNLSE Eq. (4) reads

$$H = \sum_j\left[\frac{-1}{4}\left\{\left(1-(-1)^j\alpha\right)\left(\Psi_j\Psi_{j+1}^* + \Psi_j^*\Psi_{j+1}\right) + \left(1-(-1)^{j-1}\alpha\right)\left(\Psi_j\Psi_{j-1}^* + \Psi_j^*\Psi_{j-1}\right)\right\} + \varepsilon_j\left|\Psi_j\right|^2 + \frac{\Lambda}{2}\left|\psi_j\right|^4\right], \tag{5}$$

where $\sum_j\left|\Psi_j\right|^2 = 1$. To analyze the Bloch dynamics, we study the dynamical evolution of a site-dependent Gaussian wavepacket, which we parameterize as

$$\Psi_j(t) = \sqrt{K}\exp\left[-\frac{(j-\xi)^2}{\gamma^2} + ip(j-\xi) + i\frac{\delta}{2}(j-\xi)^2 + i(-1)^j\frac{\phi}{2}\right], \tag{6}$$

where $\xi(t)$ and $\gamma(t)$ are, respectively, the center and width of the condensate, $p(t)$ and $\delta(t)$ are their associated momenta, and $K(\gamma,\xi)$ a normalization factor. Here $(-1)^j\frac{\phi}{2}$ is the phase of the wave packet at the j^{th} site. Clearly, depending upon whether j is odd or even, the phase is $\pm\frac{\phi}{2}$. As explained in [29], as the condensate moves from one well to the next, it acquires additional phase, which depends on the height of the barrier. As the height of the barrier alternates, the phase also alternates.

The dynamics of the wave packet can be obtained by the variational principle from the Lagrangian, $L = \sum_j i\Psi_j\Psi_j^* - H$, with the equations of motion for the variational parameters $q_i(t) = \xi,\gamma,p,\delta,\phi$ given by $\frac{d}{dt}\frac{\partial L}{\partial\dot{q}_i} = \frac{\partial L}{\partial q_i}$. The phase is used to enforce a constraint. The Lagrangian is

$$L = p\dot{\xi} - \frac{\gamma^2\dot{\delta}}{8} - \left[\frac{\Lambda}{2\sqrt{\pi}\gamma}\right] + \left\{\cos\phi\cos p + \alpha\sin\phi\sin p\right\}\exp(-\eta) - V(\gamma,\xi), \tag{7}$$

where $\eta = \frac{1}{2\gamma^2} + \frac{\gamma^2\delta^2}{8}$ and $V(\gamma,\xi) = K\int_{-\infty}^{\infty}dj\,\varepsilon_j\exp\left(-2\frac{(j-\xi)^2}{\gamma^2}\right)$.

The variational equations of motion are:

$$\dot{p} = -\frac{\partial V}{\partial\xi}, \tag{8a}$$

$$\dot{\xi} = \left[\cos\phi\sin p - \alpha\sin\phi\cos p\right]\exp(-\eta), \tag{8b}$$

$$\dot{\delta} = \left[\cos\phi\cos p + \alpha\sin\phi\sin p\right]\exp(-\eta)\left[\frac{4}{\gamma^4} - \delta^2\right] + \frac{2\Lambda}{\gamma^3\sqrt{\pi}} - \frac{4}{\gamma}\frac{\partial V}{\partial\gamma}, \tag{8c}$$

$$\dot{\gamma} = \gamma\delta\,[\cos\phi\cos p + \alpha\sin\phi\sin p]\exp(-\eta), \tag{8d}$$

$$\tan\phi = \alpha\tan p. \tag{8e}$$

Since $\cos^2\phi + \sin^2\phi = 1$, together with equation (8a-8e), we get the following constraints on $\cos\phi$ and $\sin\phi$:

$$\cos\phi = \frac{\cos p}{\sqrt{\cos^2 p + \alpha^2\sin^2 p}}, \tag{9a}$$

$$\sin\phi = \frac{\alpha\sin p}{\sqrt{\cos^2 p + \alpha^2\sin^2 p}}. \tag{9b}$$

Corresponding to the variational equations (8a-8e) and constraints (9a-9b) the effective Hamiltonian is written as

$$H = \frac{\Lambda}{2\sqrt{\pi}\gamma} - \cos p\sqrt{1+\alpha^2\tan^2 p}\exp(-\eta) + V(\gamma,\xi). \tag{10}$$

We first study the Bloch oscillations. For the tilted periodic potential, the on-site energies are written as $\varepsilon_j = j\omega_B$.

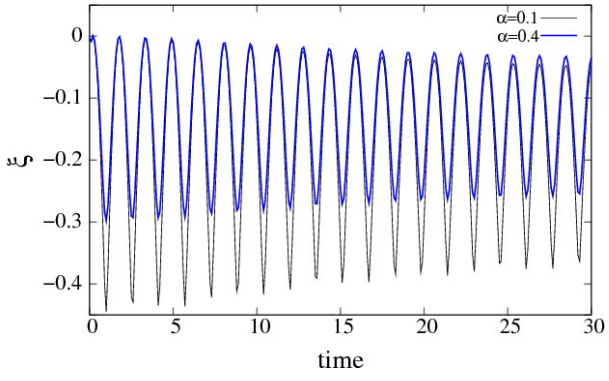

Figure 1. Oscillations of the center-of-mass $\xi(t)$ are depicted for two different values of the secondary lattice strength, $\alpha = 0.1$ and $\alpha = 0.4$. The other parameters are $\xi(0) = 0$, $p(0) = 0$, $\delta(0) = 0$, $\gamma(0) = 10$, $\Lambda = 20$, $\omega_B = 2$. On increasing the strength of the secondary lattice, the amplitude of the center-of-mass motion reduces.

Using equations (8a-8e), we find $V = \xi\omega_B$ and $\dot{p} = -\omega_B$. We solve the variational equations of motion numerically using a fifth-order Runge-Kutta method, with the initial values $\xi(0) = 0$, $p(0) = 0$, $\delta(0) = 0$, $\gamma(0) = 10$, and the parameters $\Lambda = 20$, $\omega_B = 2$. The result for the center-of-mass $\xi(t)$ is depicted in figure 1 for two different values of the secondary lattice strength, $\alpha = 0.1$ and $\alpha = 0.4$. Clearly on increasing the strength of the secondary lattice from $\alpha = 0.1$ to $\alpha = 0.4$, the amplitude of the center-of-mass motion reduces. The secondary lattice serves to break the discrete translational invariance of the system, thus favouring localization of the wave function. Optical superlattices with higher periodicities will block the center-of-mass more strongly. The observed damping (with respect to time) in fig. 1 is due to interactions. In the absence of interactions, the center of the BEC for $p_0 = 0$ goes roughly as $\xi(t) \approx -(1-\alpha^2)(1-\cos\omega_B t)$, while in the presence of interactions, the oscillations roughly decreases as $\xi(t) \approx -(1-\alpha^2)\left(1-\exp\left(-\frac{\Lambda t^2}{2\pi\gamma_f^4}\right)\cos\omega_B t\right)$. Here, γ_f is some final value of γ. Clearly, when there is no interaction, there is no damping of the Bloch oscillations in time but there is a reduction in the amplitude by a factor $(1-\alpha^2)$ due to the presence of the secondary lattice. In order to understand the origin of this blocking of the center-of-mass motion, we derive the effective mass $(m^*)^{-1} = \frac{\partial^2 H}{\partial p^2}$ as,

$$m^* = \frac{\left(1+\alpha^2\tan^2 p\right)^{3/2}\exp(\eta)}{\cos p\left(1-\alpha^2\tan^4 p\right)(1-\alpha^2)}. \tag{11}$$

A diverging effective mass $m^* \to \infty$ as $t \to \infty$ due to interactions leads to a self-trapping of the wave packet [17]. In the expression for the effective mass (Eq. 11), in the absence of interaction, the factor $\exp(\eta)$ is constant since γ tends to a final value γ_f and $\delta(t) \approx \delta_0$ (initial value). This can be seen from equations 8c and 8d. The effective mass is now enhanced due to the presence of the secondary lattice. Since $\Lambda = 0$, the effective mass stays constant in time and the Bloch oscillations show reduced oscillations compared to the case for a single frequency optical lattice but does not show damping in time. On the other hand when $\Lambda \neq 0$, and $t \to \infty$, $\gamma \to \gamma_f$ and $\delta(t) \approx \frac{2\Lambda t}{\gamma_f^3\sqrt{\pi}}$, so that $m^* \to \infty$. This causes not only a reduction in amplitude but also damping in time. It is interesting to note that, we now have an additional handle to tune the effective mass. A plot between m^* and α (for $p = 0$) in figure 2 shows that as the strength of the secondary lattice increases, the effective mass also increases. Therefore the origin of the reduction of the amplitude of Bloch oscillations of a BEC in an optical superlattice is due to an increase of the effective mass. Dynamics of localized excitations, such as solitons depends on the effective mass, hence the secondary lattice emerges as a useful additional handle to manipulate localized excitations.

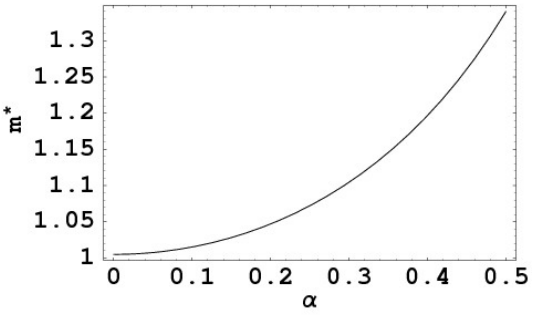

Figure 2. A plot relating m^* to α shows that, as the strength of the secondary lattice increases, the effective mass also increases. Therefore the origin of the localization of a BEC in an optical superlattice is due to an increase in the effective mass.

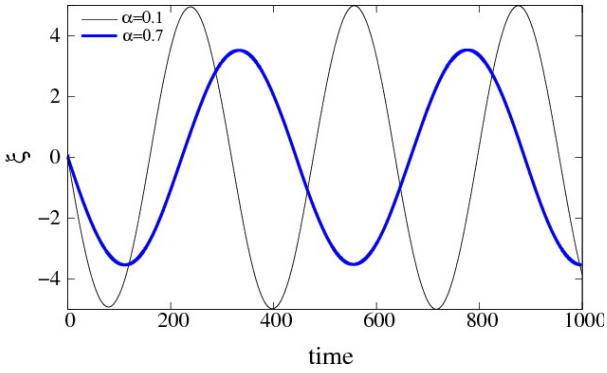

Figure 3. A plot of the dipole oscillations for $\alpha = 0.1$ and $\alpha = 0.7$. The other parameters are $\xi(0) = 0$, $p(0) = 0.1$, $\delta(0) = 0$, $\gamma(0) = 40$, $\Lambda = 5$, $\Omega = 0.0002$. We notice that, as the strength of the secondary lattice increases, the dipole oscillations are blocked in accordance with the experimental observations of [31]. Since we are in the negligible mean field interaction regime, the dipole oscillations are not damped.

3. Dipole oscillations

We study now the dipole oscillations. Instead of the gravitational potential, we consider a sufficiently large magnetic harmonic potential ($\omega_z \approx \omega_s$) superimposed on the optical lattice, $\varepsilon_j = \Omega j^2$, where $\Omega = \frac{m\omega_z^2 d^2}{J_0}$. The variational equations of motion give $V(\gamma, \xi) = \Omega\left(\frac{\gamma^2}{4} + \xi^2\right)$ and $\dot{p} = -2\Omega\xi$. In the regime of negligible mean field interaction ($\Lambda = 0$) and small momenta p, the equation for the center-of-mass is $\dot{\xi}(t) = \left(1 - \alpha^2\right)p$. Consequently, the center-of-mass obeys the equation of an undamped harmonic oscillator, $\ddot{\xi} = \omega_d^2\xi$, where the frequency of dipole oscillation, $\omega_d^2 = 2\Omega\left(1 - \alpha^2\right) = \omega_z^2\left(\frac{m}{m^*}\right)$ is reduced in the presence of the secondary lattice since $m^* > m$. We consider the initial conditions $\xi(0) = 0$ and $p(0) = p_0$. The center-of-mass in the $\Lambda = 0$ regime and small momenta is $\xi(t) \approx \frac{\left(1-\alpha^2\right)^{1/2}}{\sqrt{2\Omega}} \sin\omega_d t$. In the low momenta limit, the amplitude of the center-of-mass decreases with increasing strength of the secondary lattice approximately as $\left[1 - \left(\frac{s_2}{s_1\left(\frac{\pi^2}{2} - 2\right)}\right)^2\right]^{1/4}$. In the experiment [16], $\omega_z \approx 2\pi \times 10$ Hz and $\lambda_1 \approx 830 \times 10^{-9}$ nm. This corresponds to a very low value of $\Omega \approx 0.0001$ (in dimensionless units).

We solve the variational equations of motion numerically using the fifth-order Runge-Kutta method [32], for the following initial values: $\xi(0) = 0$, $p(0) = 0.1$, $\delta(0) = 0$, $\gamma(0) = 40$ and the parameters: $\Lambda = 5$, $\Omega = 0.0002$. The result for the dipole oscillation is depicted in figure 3 for two different values of the secondary lattice strength $\alpha = 0.1$ and $\alpha = 0.7$. For $\Lambda = 5$, we are still in the regime of negligible mean field interaction and we do not expect any damping. On increasing the strength of the secondary lattice, the amplitude of the center-of-mass $\xi(t)$ is reduced in accordance with the experiments of [31]. This reduction in the amplitude of the dipole oscillation on increasing the strength of the secondary lattice is due to an increase in the effective mass, as mentioned earlier in this paper. The initial value of the effective mass can be positive ($\cos p_0 > 0$) or negative ($\cos p_0 < 0$). Let us suppose that $\cos p_0 > 0$ and initial values: $\gamma(0) = \gamma_0$, $\delta(0) = \delta_0 = 0$ and $\xi(0) = \xi_0 = 0$. The initial value of the Hamiltonian is $H_0 = \frac{\Lambda}{2\sqrt{\pi}\gamma_0} - \cos p_0\sqrt{1 + \alpha^2\tan^2 p_0}\exp\left(-\frac{1}{2}\gamma_0^2\right) + \frac{\Omega\gamma_0^2}{4}$. Since the Hamiltonian is conserved, we have $H_0 = \frac{\Lambda}{2\sqrt{\pi}\gamma_0} - \cos p_0\sqrt{1 + \alpha^2\tan^2 p_0}\exp\left(-\frac{1}{2}\gamma^2 - \frac{\gamma^2\delta^2}{8}\right) + \frac{\Omega\gamma^2}{4}$. The parabolic external potential helps to keep $H_0 > 0$, therefore,

$$\frac{\Lambda}{2\sqrt{\pi}\gamma} + \frac{\Omega\gamma^2}{4} - H_0 > 0. \tag{12}$$

The trajectories in the $\gamma - \delta$ plane are given by

$$\delta^2 = -\frac{1}{\gamma^4}\left[8\gamma^2\log\left(\frac{\frac{\Lambda}{2\pi\gamma} + \frac{\Omega\gamma^2}{4} - H_0}{\cos p_0\sqrt{1 + \alpha^2\tan^2 p_0}}\right) + 4\right]. \tag{13}$$

Figure 4 shows a plot of the center-of-mass for $\alpha = 0.1$, $\xi(0) = 0$, $p_0 = 0.1$, $\delta_0 = 0.1$, $\gamma_0 = 10$, $\Lambda = 47,57$, $\omega = 0.0002$. We notice that for such high values of Λ, the dipole oscillations are completely blocked. Both interactions and secondary lattice induced disorder cooperate to block the center-of-mass motion. For the higher value of Λ, the center-of-mass stops at an earlier time, which again is in accordance with experiments [31]. From equation (13), we notice that $\delta \to \infty$ as $t \to \infty$. Therefore, for large time,

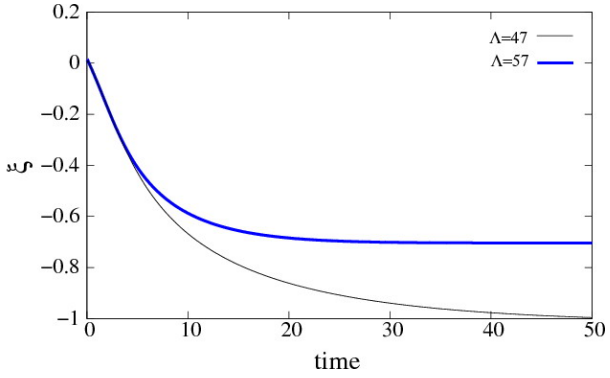

Figure 4. Center-of-mass motion for $\alpha = 0.1$, $\xi(0) = 0$, $p_0 = 0.1$, $\delta_0 = 0.1$, $\gamma_0 = 10$, $\Lambda = 47, 57$, $\omega = 0.0002$. We notice that for such high values of Λ, the dipole oscillations are completely blocked. Both interactions and secondary lattice induced disorder cooperate to block the center-of-mass motion.

$$\dot{\xi} \approx (1-\alpha^2)\sin p_0 \exp\left(-\frac{1}{2\gamma_{max}^2} - \frac{\gamma_{max}^2\delta^2}{8}\right) \to 0 \quad (14)$$

and

$$m^* = \frac{\left(1+\alpha^2\tan^2 p\right)^{3/2}\exp\left(\frac{1}{2\gamma_{max}^2}+\frac{\gamma_{max}^2\delta^2}{8}\right)}{\cos p\left(1-\alpha^2\tan^4 p\right)(1-\alpha^2)} \to \infty. \quad (15)$$

The center of the BEC wavepacket stops and the effective mass goes to infinity and there is an energy transfer from the kinetic energy to the internal modes, since δ is the momentum associated with the width γ. This is the self-trapped regime. We also find that the final value of center-of-mass ξ_f is not the same as ξ_0. For a fixed Λ, an increase in the secondary lattice potential will block the center-of-mass at an earlier time.

4. Conclusions

For Bose-Einstein condensates trapped in an optical superlattice, the addition of the secondary lattice blocks centre-of-mass motion. This is due to an increase in effective mass. Adding the secondary lattice also reduces the dipole oscillation frequency. These results agree with recent experiments [31]. We found the secondary lattice useful for theoretically investigating and manipulating localized excitations.

Acknowledgments

Aranya Bhattacherjee acknowledges a fellowship from the German Academic Exchange Service (DAAD) (A/06/33410); is grateful to Professor R. Graham for facilities to carry out part of this work at the University of Duisburg-Essen, Germany; and thanks the Max Planck Institute for Physics of Complex Systems, Dresden, Germany for its hospitality. Monika Pietrzyk acknowledges support for Project D20 in the DFG Research Center Matheon "Mathematics for key technologies" in Berlin.

References

[1] O. Morsch, M. Oberthaler, Rev. Mod. Phys. 78, 179 (2006)
[2] B.P. Anderson, M. A. Kasevich, Science 282, 1686 (1998)
[3] C. Orzel, A.K. Tuchman, M.L. Fenselau, M. Yasuda, M.A. Kasevich Science,291 , 2386 (2001)
[4] O. Morsch, J.H. Müller, M. Cristiani, D. Ciampini, E. Arimondo, Phys. Rev. Lett. 87, 140402 (2001)
[5] M. Greiner, O. Mandel, T. Esslinger, T.W. Hänsch, I. Bloch, Nature 415, 39 (2002)
[6] A.R. Kolovsky, Phys. Rev. Lett. 90, 213002 (2003)
[7] A.R. Kolovsky, J. Korsch, Phys. Rev. A 67, 063601 (2003)
[8] B.M. Breid, D. Witthaut, H.J. Korsch, New J. Phys. 8, 110 (2006)
[9] A. Trombettoni, A. Smerzi, Phys. Rev. Lett. 86, 2353 (2001)
[10] J.C. Eilbeck et al., In: L. Vazquez, R.S. MacKay, M.P. Zorzano (Eds.), Localization and Energy Transfer in Nonlinear Systems (World Scientific, Singapore, 2003) 44
[11] R. Livi , R. Franzosi, G-L. Oppo, Phys. Rev. Lett. 97, 060401 (2006)
[12] Th. Anker et al., Phys. Rev. Lett. 94, 020403 (2005)
[13] R. Gati, B. Hemmerling, J. Foelling, M. Albiez, M.K. Oberthaler, Phys. Rev. Lett. 96, 130404 (2006)
[14] M. Albiez, R. Gati, J. Foelling, S. Hunsmann, M. Cristiani, M.K. Oberthaler, Phys. Rev. Lett. 97, 010405 (2005)
[15] S. Raghavan, A. Smerzi, S. Fantoni1, S. R. Shenoy, Phys. Rev. A 59, 620 (1999)
[16] R. Franzosi, V. Penna, Phys. Rev. A 65, 013601 (2001)
[17] B. Liu, L-B. Fu, S-P. Yang, J. Liu, Phys. Rev. A 75, 033601 (2007)
[18] J. Sebby-Strabley et al., Phys. Rev A 73, 033605 (2006)
[19] S. Peil et al., Phys. Rev. A. 67, 051603 (R) (2003)

[20] P. Buonsante, A. Vezzani, Phys. Rev. A 70, 033608 (2004)
[21] P.J.Y. Louis, E. A. Ostrovskaya, Y.S. Kivshar, J. Opt. B 6, S309 (2004)
[22] P.J.Y. Louis, E. A. Ostrovskaya, Y.S. Kivshar, Phys. Rev. A 71, 023612 (2005)
[23] L.A. Dmitrieva, Y.A. Kuperin, arXiv:cond-mat/0311468
[24] A.M. Rey, B.L. Hu, E. Calzetta, A. Roura, C.W. Clark, Phys. Rev. A 69, 033610 (2004)
[25] R. Roth, K. Burnett, Phys. Rev. A 68, 023604 (2003)
[26] M.A. Porter, P.G. Kevrekidis, R. Carretero-Gonzalez, D.J. Frantzeskakis, Phys. Letts. A 352, 210 (2006)
[27] C-C. Huang, W-C. Wu, Phys. Rev. A 72, 065601 (2005)
[28] V.G. Rousseau et al., Phys. Rev. B 73, 174516 (2006)
[29] A. Bhattacherjee, J. Phys. B-At. Mol. Opt. 40, 143 (2007)
[30] A. Bhattacherjee, Eur. Phys. J. D 46, 499 (2008)
[31] J.E. Lye et al., Phys. Rev. A 75, 061603 (2007)
[32] W.H. Press, S.A. Teukolsky. W.T. Vetterling, B P. Flannery, Numerical Recipes in Fortran 77 (Cambridge University Press, Cambridge, 1992) 16.2